

Numerical Heat Transfer, Part A: Applications

An International Journal of Computation and Methodology

ISSN: (Print) (Online) Journal homepage: <https://www.tandfonline.com/loi/unht20>

Heat transfer optimisation through viscous ternary nanofluid flow over a stretching/shrinking thin needle

Liping Yu, Yijie Li, Venkatesh Puneeth, Sami Znaidia, Nehad Ali Shah, Sarpabhushana Manjunatha, Muhammad Shoaib Anwar & Muhammad Riaz Khan

To cite this article: Liping Yu, Yijie Li, Venkatesh Puneeth, Sami Znaidia, Nehad Ali Shah, Sarpabhushana Manjunatha, Muhammad Shoaib Anwar & Muhammad Riaz Khan (26 Oct 2023): Heat transfer optimisation through viscous ternary nanofluid flow over a stretching/shrinking thin needle, Numerical Heat Transfer, Part A: Applications, DOI: [10.1080/10407782.2023.2267750](https://doi.org/10.1080/10407782.2023.2267750)

To link to this article: <https://doi.org/10.1080/10407782.2023.2267750>



© 2023 The Author(s). Published with license by Taylor & Francis Group, LLC



Published online: 26 Oct 2023.



Submit your article to this journal [↗](#)



Article views: 195



View related articles [↗](#)



View Crossmark data [↗](#)

Heat transfer optimisation through viscous ternary nanofluid flow over a stretching/shrinking thin needle

Liping Yu^a, Yijie Li^b, Venkatesh Puneeth^c , Sami Znaidia^d, Nehad Ali Shah^e, Sarpabhushana Manjunatha^f, Muhammad Shoab Anwar^g, and Muhammad Riaz Khan^h

^aSchool of Computer Science and Technology, Shandong Technology and Business University, Yantai, China;

^bSchool of Computer Science, University of St. Andrews, UK; ^cSchool of Sciences, CHRIST University,

Ghaziabad, India; ^dDepartment of Physics, College of Sciences and Arts in Mahayel Asir, King Khalid

University, Abha, Saudi Arabia; ^eDepartment of Mechanical Engineering, Sejong University, Seoul, South

Korea; ^fDepartment of Sciences and Humanities, CHRIST University, Bengaluru, India; ^gDepartment of

Mathematics, University of Jhang, Pakistan; ^hDepartment of Mathematics, Quaid-i-Azam University, Islamabad, Pakistan

ABSTRACT

The current investigation interprets the flow and the thermal characteristics of the ternary nanofluid composed of MoS_2 , ZnO , and SiO_2 spherical nanoparticles and water. The resulting nanofluid is $MoS_2 - ZnO - SiO_2 - (H_2O + EG)$ where $(H_2O + EG)$ act as the base fluid which help in the flow and the nanoparticles contribute to enhancing the heat conductivity. The flow is assumed to occur across a thin needle whose surface is maintained at a higher temperature than the surroundings. The mathematical model is framed by incorporating radiation introduced by Rosseland in terms of partial differential equations (PDE). This system of equations governs the flow and thermal properties of fluid which are converted to a system of ordinary differential equations (ODE). The major outcomes of the study indicated that the increase in the amount of molybdenum disulfide enhanced the heat conducted by the nanofluid whereas it reduced the flow speed. The positive values of the heat source/sink parameter caused the heat conduction of the nanofluid to go high.

ARTICLE HISTORY

Received 2 June 2023

Revised 13 September 2023



Accepted 27 September 2023

KEYWORDS

Heat transfer; nanoparticles; radiation; slip; ternary nanofluid

1. Introduction

Nanofluids, a fascinating and rapidly evolving field of research, represent a promising class of engineered fluids that have gained substantial attention in recent years. Comprised of a base fluid combined with nanoparticles at the nanoscale, nanofluids deliver enhanced mechanical, thermal, and optical properties than their base counterparts. This amalgamation of nanotechnology and fluid dynamics has opened up new avenues for various industrial applications, ranging from advanced heat transfer systems to innovative cooling technologies. Some of the instances where nanofluids are highly influential include heat transfer and thermal management, electronics and microsystems, energy conversion and storage, oil and gas industries, automotive and aerospace, textiles and Fabrics, construction and building materials, environmental applications etc. In this regard, the analysis performed by Waqas *et al.* [1] on the nanofluid highlighted that the fluid

CONTACT Yijie Li  yjliyt@hotmail.com  School of Computer Science, University of St. Andrews, St. Andrews KY16 9AJ, UK.

© 2023 The Author(s). Published with license by Taylor & Francis Group, LLC

This is an Open Access article distributed under the terms of the Creative Commons Attribution License (<http://creativecommons.org/licenses/by/4.0/>), which permits unrestricted use, distribution, and reproduction in any medium, provided the original work is properly cited. The terms on which this article has been published allow the posting of the Accepted Manuscript in a repository by the author(s) or with their consent.

Nomenclature

α	thermal diffusivity (m^2s^{-1})	Pr	Prandtl number
δ	dimensionless thickness parameter	Q	dimensionless heat source/sink
κ	thermal conductivity ($Wm^{-1}K^{-1}$)	Q_0	heat source/sink
λ	stretching parameter	q_r	thermal radiation
μ	dynamic viscosity ($kgm^{-1}s^{-1}$)	R	dimensionless radiation
ν	kinematic viscosity (m^2s^{-1})	T	temperature (K)
ρ	density (kgm^{-3})	T_0	temperature at $y=0$ (K)
(u, v)	velocity components (ms^{-1})		
σ^*	Stefan Boltzmann constant		
C_{f_x}	skin friction coefficient		
C_p	specific heat capacity ($Jkg^{-1}K^{-1}$)		
k^*	mean absorption coefficient		
Nu_x	Nusselt number		
		Subscripts	
		f	fluid
		nf	nanofluid
		s	nanoparticle

flows faster with a higher Deborah number. The experiment designed by Javadpour *et al.* [2] concluded that the nanofluid having 0.069wt% of MWCNT with a flow rate of 2.092kg/min is an optimum setup for achieving effective cooling. Mohammadpour *et al.* [3] discussed the momentum of the fluid flow in the microchannel having protrusions in the double synthetic jets. The symmetrical analysis performed by Yaseen *et al.* [4] concluded that the $MoS_2 - SiO_2/H_2O - C_2H_6O_2$ hybrid nanofluid had an enhanced Nusselt number than $MoS_2 - H_2O$ nanofluid at the lower plate of the horizontal channel. Ali *et al.* [5, 6] discussed the impact of gravity modulation and magnetic dipole effects on the dynamics of the micropolar fluid. Anandika *et al.* [7] designed a multilayer model to optimize the heat conducted by the nanofluid. Xin *et al.* [8] discussed the impact of Thompson and Troian slips for the velocity of the nanofluid at the boundary layer. Alharbi *et al.* [9] incorporated the Cattaneo–Christov heat flux model to analyze the heat transfer characteristics of water having the suspensions of Cu nanoparticles. Khan *et al.* [10] analyzed the significance of suspending alumina nanoparticles for enhancing the thermal properties of water flowing in a vertical tube. Puneeth *et al.* [11] observed that the blade shaped nanoparticles helped in conducting more heat than any other shape of the nanoparticles in Casson hybrid nanofluid.

The enhanced thermal properties of nanofluids have increased the use of nanofluids in many industries. Hence, with the constant growth rate in the industries, the demand for nanofluids or other heat carriers increased rapidly. In this regard, the concept of ternary nanofluid was introduced which contains the suspension of 3 different nanoparticles. Each of these nanoparticles has a prominent role in acting on the heat conduction capability of the base fluid and its chemical stability. Apart from various experimental works [12–15], the theoretical model of ternary nanofluid was introduced by Manjunatha *et al.* [16, 17]. Arif *et al.* [18] compared the performance of ternary nanofluids having different shapes of particles in effectively cooling a heated system. Shahzad *et al.* [19] performed second-order convergence analysis to analyze the motion of ternary nanofluid across a spinning disk under the influence of Hall current. It was observed that the heat conducted by $Al_2O_3 - TiO_2 - CuO/H_2O$ nanofluid increased for higher ranges of radiation parameters in the study conducted by Puneeth *et al.* [20]. Wang *et al.* [21] examined the feasibility of ternary nanofluid in effective heat transfer in cooling electronic devices. Ahmed *et al.* [22] studied the $ZnO + Al_2O_3 + TiO_2/DW$ ternary nanofluid which is a sonochemically synthesized metal oxide to analyze its heat transfer properties in a square flow. A numerical study was made by Hasnain *et al.* [23] to observe the growth in the heat conducted due to the suspension of three differently shaped nanoparticles. Puneeth *et al.* [24] concluded that the temperature detected in the ternary nanofluid was higher for the high thermophoresis. Ali *et al.* [25] further analyzed the importance of bioconvection in the heat transfer analysis of nanofluid by designing the Falkner–Skan model for the flow of Maxwell nanofluid.

The thin needle is a geometric surface whose body is identified as a long and narrow cylinder with a sharp end point. A needle whose surface/body thickness becomes smaller than the boundary layer is identified as a thinner needle. The flow over such a surface (thin needle) has grabbed the interest of many scholars worldwide due to its continuous availability in electrical devices, geothermal power generation, hot wire anemometers etc. For instance, by implementing the cross-diffusion model, Rehman *et al.* [26] examined the Soret and Dufour impact on the transfer of energy and transfer mass transfer in the nanofluid flowing over the needle. Further, this study was continued by Shafiq *et al.* [27] to implement the artificial neural network. Nazar *et al.* [28] performed stability analysis to check the stability of gold-suspended nanofluid flowing past a moving needle. Meanwhile, Yasir *et al.* [29] also obtained dual solutions to study the stability of the nanofluid suspended with carbon nanotubes. Khan *et al.* [30] discussed the bioconvection activated flow of water-based hybrid nanofluid considering the chemical reaction parameter which actively influences the mass transfer profile. Puneeth *et al.* [31] studied the fourth-degree of autocatalysis that occurred in the nanofluid set to motion past a thin needle. Akinshilo *et al.* [32] observed a decrease in the velocity of the flow for the higher porosity parameter of the needle. The prominent factors such as the radiation and viscous dissipation were analyzed by Jahan *et al.* [33] on the non-isothermal flow of nanofluid across a thin needle.

$MoS_2 - ZnO - SiO_2$ refers to a composite material that is composed of Molybdenum disulfide (MoS_2), Zinc oxide (ZnO), and Silicon dioxide (SiO_2). This combination offers synergistic properties and functionalities that are not present in the individual components. The specific applications and the properties of this composition are dependent on the ratios of the components, the fabrication process, and the intended use. A thorough literature survey was performed to arrive at the research gap and it was noticed that most of the scholarly contributions to the field of nanofluids were regarding the analysis of the thermal properties of nanofluids. These contributions of scholars motivated many researchers to extend the study of nanofluids to a new concept of hybrid and ternary nanofluids having multiple suspensions of nanoparticles. Also, many articles available in the field of study discuss the heat conduction performance of hybrid nanofluids. But the volumetric analysis of the ternary nanofluid flowing past a thin needle is rarely available. Thus, this article tries to implement the Newtonian viscosity model and the Maxwell thermal conductivity model to analyze the flow and energy transfer properties of $MoS_2 - ZnO - SiO_2 - (H_2O + EG)$ ternary nanofluid. Finally, the solutions to the system of equations were obtained through the RKF-45 method, and the obtained graphical results are interpreted rigorously in this article.

2. Mathematical description and model

The laminar flow of $MoS_2 - ZnO - SiO_2 - H_2O - EG$ ternary nanofluid in two-dimensions is considered to flow over a thin needle of varying radius as shown in Figure 1. The $H_2O - EG$ mixture is in the ratio 80 : 20 whose viscosity upon suspending the nanoparticles is designed by considering the Newtonian viscosity model. The temperature of the medium is set to T_∞ while on the surface, the temperature is assumed to be T_w such that $T_w > T_\infty$. The uniform-sized spherical MoS_2 , ZnO , and SiO_2 nanoparticles are suspended in H_2O to form the ternary nanofluid flowing at a constant speed of U_∞ . The agglomeration impact is not considered since a stable nanoparticle suspension is assumed in the formation of the $MoS_2 - ZnO - SiO_2 - (H_2O + EG)$ ternary nanofluid. The thermophysical constants of the constituents of this combination are mentioned in Table 1. The energy equation is designed by using Maxwell's thermal conductivity model and heat source/sink parameter. Taking into account, the optical dense property of the mixture of water and ethylene glycol, the Rosseland approximation is implemented for modeling the thermal radiation as follows:

$$q_r = -\frac{4\sigma^* \partial T^4}{3k^* \partial r} \quad (1)$$

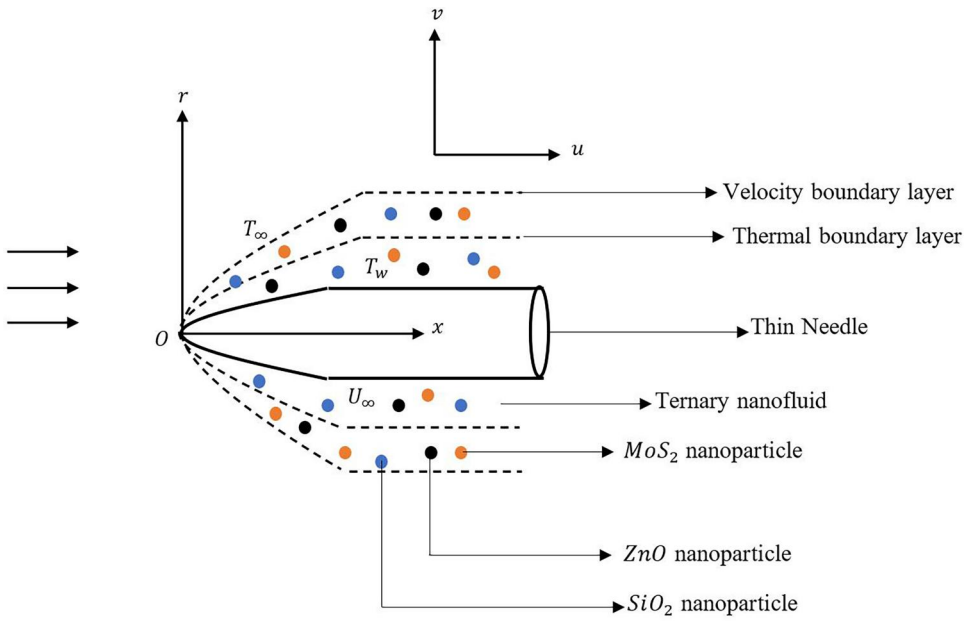


Figure 1. Flow configuration.

Table 1. The thermophysical constants of the constituents [4, 34].

Nanoparticle	ρ	C_p	κ
ZnO	5600	495.2	13
MoS ₂	5060	397.21	34.5
SiO ₂	2650	730	1.5
H ₂ O + EG	1056	3288	0.425

These assumptions lead to the formation of the following system of partial differential equations [28]:

$$\frac{\partial(ru)}{\partial x} + \frac{\partial(rv)}{\partial r} = 0 \tag{2}$$

$$u \frac{\partial u}{\partial x} + v \frac{\partial u}{\partial r} = \nu_{tf} \frac{1}{r} \frac{\partial}{\partial r} \left(r \frac{\partial u}{\partial r} \right) \tag{3}$$

$$u \frac{\partial T}{\partial x} + v \frac{\partial T}{\partial r} = \alpha_{tf} \frac{1}{r} \frac{\partial}{\partial r} \left(r \frac{\partial T}{\partial r} \right) - \frac{1}{(\rho C_p)_{tf}} \frac{\partial q_r}{\partial r} + \frac{Q_0}{(\rho C_p)_{tf}} (T - T_\infty) \tag{4}$$

The energy equation reduces to the following expression after substituting the expression of q_r in (4)

$$u \frac{\partial T}{\partial x} + v \frac{\partial T}{\partial r} = \alpha_{tf} \frac{1}{r} \frac{\partial}{\partial r} \left(r \frac{\partial T}{\partial r} \right) + \frac{16\sigma^* T_\infty^3}{3k^*(\rho C_p)_{tf}} \frac{\partial^2 T}{\partial r^2} + \frac{Q_0}{(\rho C_p)_{tf}} (T - T_\infty) \tag{5}$$

The flow is subjected to the following boundary conditions:

$$\begin{aligned} u &= U_\infty \lambda, & v &= v_w, & T &= T_w & \text{at } r &= R(x) \\ u &\rightarrow U_\infty, & T &\rightarrow T_\infty & \text{as } r &\rightarrow \infty \end{aligned} \tag{6}$$

The physical quantities of interest, especially the skin friction coefficient and the Nusselt numbers are defined as:

$$Cf_x = \frac{\mu_{tf} \left(\frac{\partial u}{\partial r} \right)_{r=R(x)}}{\rho_f U_\infty^2}, \quad Nu_x = -x \frac{\left(\kappa_{tf} \frac{\partial T}{\partial z} + q_r \right)_{r=R(x)}}{\kappa_f (T_w - T_\infty)} \quad (7)$$

The system (2)–(5) and the surface constraints (6) are converted into a system of ODEs by implementing the following relations:

$$\eta = \frac{U_\infty r^2}{\nu_f x}, \quad u = 2U_\infty f', \quad v = -\frac{\nu_f}{r} (f - \eta f'), \quad v_w = -\frac{\nu_f \lambda}{r} \delta, \quad \theta = \frac{T - T_\infty}{T_w - T_\infty} \quad (8)$$

Upon setting the value of $\eta = \delta$ in Eq. (6) which signifies the wall of the needle, the surface of the needle shall be defined as

$$R(x) = \sqrt{\frac{\nu_f \delta x}{U_\infty}} \quad (9)$$

The continuity equation (Eq. (2)) is satisfied for the similarity transformation defined above in (8) and the resulting system equations are of the form:

$$\frac{\mu_{tf}}{\mu_f} \left(\eta f'' + f'' \right) + 0.5 \frac{\rho_{tf}}{\rho_f} f f'' = 0 \quad (10)$$

$$\left(\frac{\kappa_{tf}}{\kappa_f} + \frac{4}{3} R \right) \eta \theta'' + \frac{\kappa_{tf}}{\kappa_f} \theta' + Pr \left[0.25 Q \theta + \frac{(\rho C p)_{tf}}{(\rho C p)_f} f \theta' \right] = 0 \quad (11)$$

The boundary conditions corresponding to (6) take the following form:

$$f'(\delta) = \frac{\lambda}{2}, \quad f(\delta) = \lambda \delta, \quad \theta(\delta) = 1, \quad f'(\infty) \rightarrow 0.5, \quad \theta'(\infty) \rightarrow 0 \quad (12)$$

The nondimensionalized expression for Cf_x (skin friction coefficient) and Nu_x (Nusselt number) takes the following form:

$$\frac{Cf_x \sqrt{Re_x}}{4\sqrt{\delta}} = \frac{\mu_{tf}}{\mu_f} f''(0), \quad \frac{Nu_x}{2\sqrt{\delta} Re} = -\left(\frac{\kappa_{tf}}{\kappa_f} + \frac{4}{3} R \right) \theta'(0) \quad (13)$$

The nondimensional parameters appearing in this model are expressed as follows:

$$Q = \frac{Q_0 x}{U_\infty (\rho C p)_f}, \quad Pr = \frac{\nu_f}{\alpha_f}, \quad R = \frac{4\sigma^* T_\infty^3}{k^* \alpha_f}, \quad Re_x = \frac{x U_\infty}{\nu_f}$$

3. Thermophysical and rheological properties

The rheological and thermophysical properties of the ternary nanofluids are stated below [16]:

1. Density:

$$\rho_{tf} = (1 - \phi_3) \{ (1 - \phi_2) [(1 - \phi_1) \rho_f + \phi_1 \rho_1] + \phi_2 \rho_2 \} + \phi_3 \rho_3.$$

2. Viscosity

$$\mu_{tf} = \frac{\mu_f}{(1 - \phi_1)^{2.5} (1 - \phi_2)^{2.5} (1 - \phi_3)^{2.5}}.$$

3. Specific heat capacity:

$$(\rho Cp)_{tf} = (1 - \phi_3)\{(1 - \phi_2)[(1 - \phi_1)(\rho Cp)_f + \phi_1(\rho Cp)_1] + \phi_2(\rho Cp)_2\} + \phi_3(\rho Cp)_3.$$

4. Thermal conductivity

$$\frac{\kappa_{tf}}{\kappa_{hmf}} = \frac{\kappa_3 + 2\kappa_{hmf} - 2\phi_3(\kappa_{hmf} - \kappa_3)}{\kappa_3 + 2\kappa_{hmf} + \phi_3(\kappa_{hmf} - \kappa_3)},$$

where $\frac{\kappa_{hmf}}{\kappa_f} = \frac{\kappa_2 + 2\kappa_{hmf} - 2\phi_2(\kappa_{hmf} - \kappa_2)}{\kappa_2 + 2\kappa_{hmf} + \phi_2(\kappa_{hmf} - \kappa_2)}$ and $\frac{\kappa_f}{\kappa_1} = \frac{\kappa_1 + 2\kappa_f - 2\phi_1(\kappa_f - \kappa_1)}{\kappa_1 + 2\kappa_f + \phi_1(\kappa_f - \kappa_1)}$.

4. Solution methodology

The RKF-45 method, also known as the Runge-Kutta-Fehlberg method, is a numerical integration technique used to solve ordinary differential equations (ODEs). It is an adaptive step-size method that provides a compromise between accuracy and computational efficiency. It combines two different Runge-Kutta methods of different orders to estimate the solution and an error estimate. The error estimate is then used to adaptively adjust the step size for improved accuracy. The convergence criteria of RKF-45 involve comparing the solutions obtained using the fourth-order and fifth-order methods and using an error estimate to control the step size. This method is widely used in scientific and engineering applications where numerical integration of ODEs is required. Its adaptive nature makes it suitable for solving ODEs with varying behaviors, such as stiff systems or systems with rapid changes in dynamics. Thus, the altered governing equations (10)–(12) are converted into an initial value problem and the RKF-45 method is implemented through maple to obtain the solution with an accuracy of 10^{-5} . Due to these advantages, many authors [35–38] have used RKF-45 method to perform the analysis. In order to apply the RKF-45 method to the system of Eqs. (10)–(12), it must be converted to initial value problem that can be done by using the following transformation:

$$\begin{pmatrix} f & f' & f'' & f''' \\ \theta & \theta' & \theta'' & 0 \end{pmatrix} = \begin{pmatrix} D_1 & D_2 & D_3 & D'_3 \\ D_4 & D_5 & D'_5 & 0 \end{pmatrix} \quad (14)$$

Upon using the above transformations, the system of equations reduces to the following form:

$$\begin{pmatrix} D'_1 \\ D'_2 \\ D'_3 \\ D'_4 \\ D'_5 \end{pmatrix} = \begin{pmatrix} D_2 \\ D_3 \\ \frac{1}{\eta} \left[\frac{\mu_f}{\mu_{tf}} \left(-0.5 \frac{\rho_{tf}}{\rho_f} D_1 D_2 \right) - D_3 \right] \\ D_5 \\ -\frac{1}{\eta} \left[\frac{\kappa_{tf}}{\kappa_f} + \frac{4}{3} R \right]^{-1} \left[\frac{\kappa_{tf}}{\kappa_f} D_5 + Pr \left(0.25 Q D_4 + \frac{(\rho Cp)_{tf}}{(\rho Cp)_f} D_1 D_5 \right) \right] \end{pmatrix} \quad (15)$$

Subject to the constraints:

$$D_1(\delta) = \lambda \delta, \quad D_2(\delta) = \frac{\lambda}{2}, \quad D_3(\delta) = a_1, \quad D_4(\delta) = 1, \quad D_5(\delta) = a_2 \quad (16)$$

In the above problem, a_1 , a_2 , and a_3 are positive constants. The obtained results are verified as shown in Table 2 by referring to the existing literature.

Table 2. Validating the obtained results through comparison.

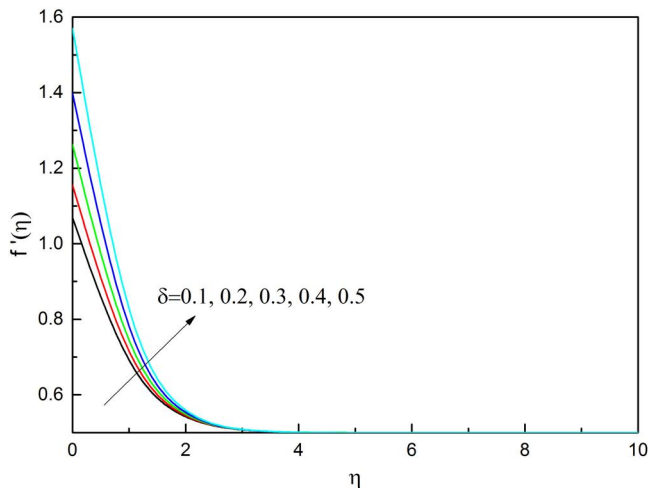
Pr	Qasim et al. [39]	Suleman et al. [40]	Present
		$-\theta'(0.1)$	
0.72	1.23664	1.23665	1.23666
1	1.0000	1.00000	0.99999
6.7	0.3333	0.3331	0.3336
10	0.26876	0.26877	0.26877

5. Result analysis

Due to the advantages listed above, the RKF-45 approach and the shooting method are used to solve the dimensionless system of Eqs. (10)–(12). Graphs and tables are used to discuss the analysis of the flow's parameters. The Prandtl number (Pr) is kept constant at 6.7 for this study since it is assumed that the base fluid is a Newtonian fluid, and the overall nanoparticle volume fraction (ϕ) is maintained at 0.03 to prevent the potential of sedimentation.

The graphical analysis of the impact of the thickness of the needle is shown in Figure 2 according to which an increase in the velocity profile is observed. The increase in the δ corresponds to the increase in the width/opening of the needle as it is directly linked with the radius. As the value of this parameter is increased, it widens the gap and allows more space for the flow of fluid. As a result, a huge amount of nanofluid flows in a shorter duration of time. Similarly, the impact of the same parameter on the temperature of the nanofluid is seen in Figure 3. Since the fluid flows faster and the quantity of fluid within the region of the needle increases with the increase in δ , the heat conducted by the nanofluid gets distributed between the nanofluid layers and thus a lower temperature is recorded. The existence of the heat sink/source has played a significant impact on the temperature of the nanofluid and this impact is shown in Figures 4 and 5. The parameter Q is responsible for analyzing this effect and it acts as a heat source when $Q > 0$ and acts as a heat sink when $Q < 0$. The increase in the positive values of Q signifies that more heat is being emitted from the source which is absorbed by the nanofluid and thus an enhancement in the temperature is recorded. Similarly, an action of a strong heat sink is obtained for lower values of Q which the excess heat and thus reduces the temperature of the nanofluid.

It is important to note that the effect of radiation on the temperature of a nanofluid can be complex and depends on several factors, including the properties of the nanoparticles, the concentration of nanoparticles, the temperature of the fluid, and the radiation source. Detailed


Figure 2. δ influence on $f'(\eta)$.

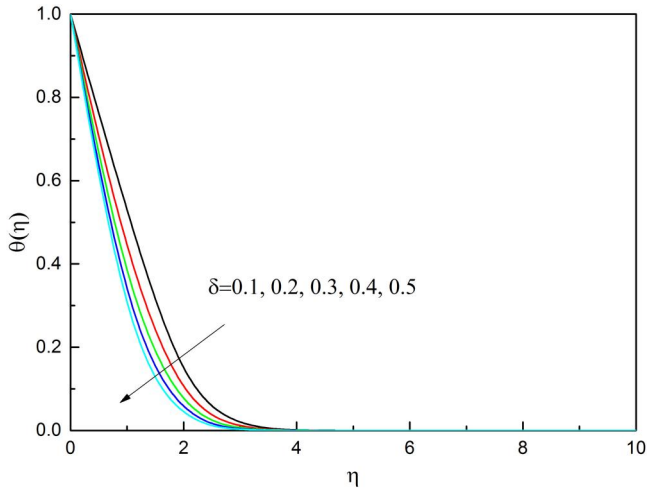


Figure 3. δ influence on $\theta(\eta)$.

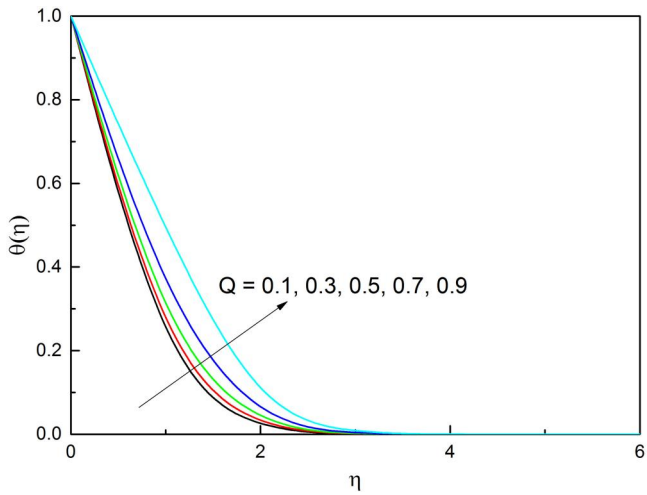


Figure 4. Q influence on $\theta(\eta)$.

analysis and modeling are often required to understand and quantify the specific impact of radiation on the temperature behavior of a nanofluid in a given application. Figure 6 depicts the influence of thermal radiation on the temperature of the nanofluid. An increase in the nanofluid's temperature is noted for higher values of R . This enhancement in the temperature is observed due to the absorption of heat emitted from the surface by the nanofluid. Overall, radiation can contribute to the heat transfer and temperature of a nanofluid, and its influence should be considered alongside other modes of heat transfer, such as conduction and convection when studying or utilizing nanofluids in various thermal systems.

Nanofluids with different nanoparticle volume fractions exhibit varying flow behaviors. At low-volume fractions, nanofluids may flow similarly to their base fluids. However, as the volume fraction increases, the presence of nanoparticles can alter the flow characteristics, leading to changes in viscosity, rheology, and pressure drop. It's worth noting that the optimal nanoparticle volume fraction varies depending on the specific application and the desired property enhancement. Hence, significant analysis is made to understand the impact of the nanoparticle volume

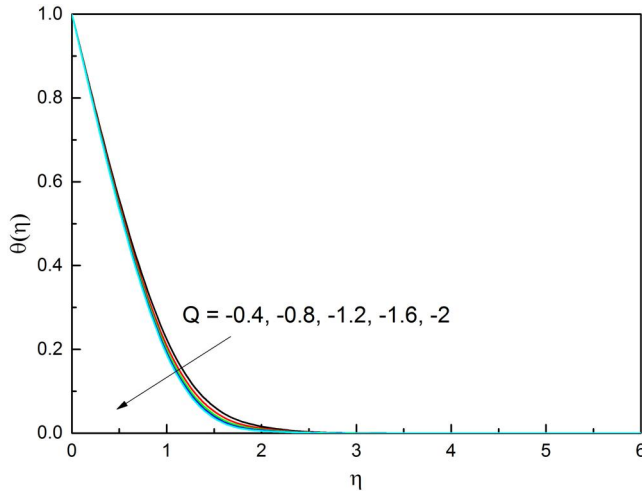


Figure 5. Q influence on $\theta(\eta)$.

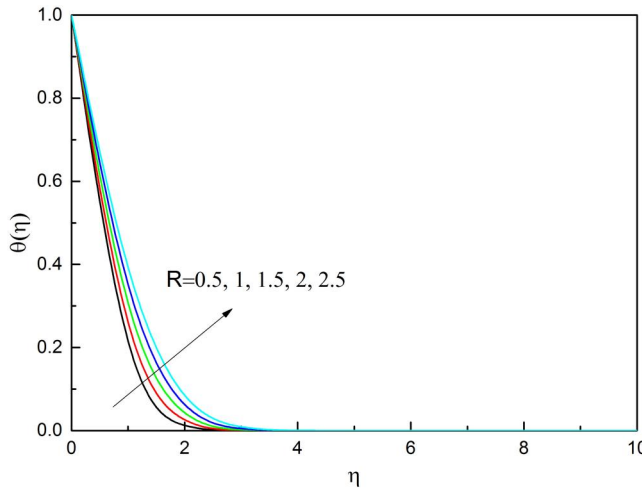


Figure 6. R influence on $\theta(\eta)$.

fraction of MoS_2 (ϕ_3) on the velocity and temperature. The volume fraction parameter ϕ_3 is directly linked to the number of nanoparticles that are being suspended in the nanofluid. Thus, the analysis of this parameter has a significant role in the model. Hence, the examination of the impact of ϕ_3 on the flow of the nanofluid is performed by the values of $\phi_1 = \phi_2 = 0.0025$ so that the overall volume fraction does not exceed 0.03 and the same is depicted in Figure 7. It is observed that as the volume proportion of nanoparticles grows, so does the density of the nanofluid, which lowers the velocity of the nanofluid. The thermal conductivity of the nanofluid will increase with the volume percentage of nanoparticles. Consequently, the temperature of the nanofluid rises as the volume percentage of nanoparticles increases as depicted in Figure 8. Different studies and applications may have different recommended ranges of volume fraction based on the target performance and stability requirements. Therefore, it is important to consider the specific needs and constraints of the application when determining the appropriate nanoparticle volume fraction for a given nanofluid.

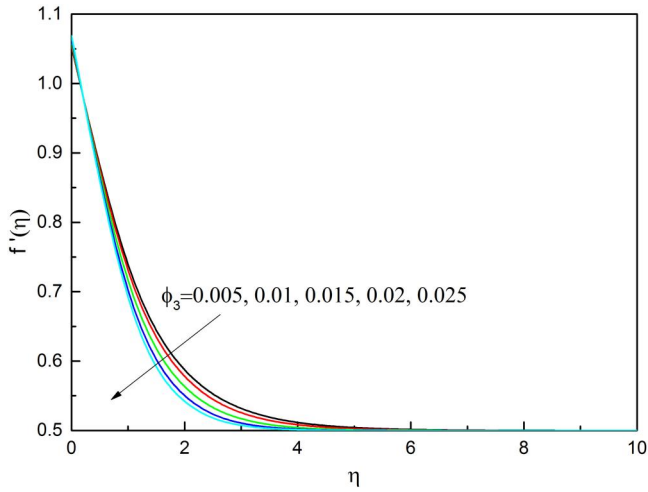


Figure 7. ϕ_3 influence on $f'(\eta)$.

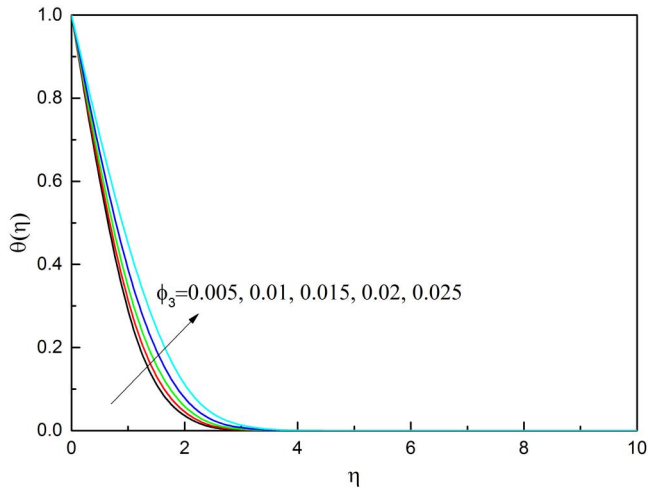


Figure 8. ϕ_3 influence on $\theta(\eta)$.

The role of the stretching parameter λ on the velocity profile is depicted in [Figures 9](#) and [10](#). It is observed that the velocity of the flow increases for higher values of λ because of the fact that the positive values indicate stretching. The increase in the positive values of λ indicates faster stretching and due to the adhesive force between the layer of fluid and the surface, the nanofluid gets pulled along the surface, and hence an increase in the velocity is noted. In the case of the negative values of λ , the needle is assumed to shrink which creates a drag that opposes the fluid flow. Thus, a reduction in the velocity is seen as the values of λ take lower values. Further, due to the high-speed flow that occurs because of the fast stretching, the heat absorption capacity of the nanofluid cannot reach its maximum capacity thus, a drop in the temperature is seen for higher values of λ as depicted in [Figures 11](#) and [12](#).

The influence of the fluid parameters on the skin friction coefficient (C_{f_x}) and the Nusselt number (Nu_x) is tabulated in [Table 3](#). Skin friction is found to increase with the rise in the volume fraction parameter whereas the Nusselt number is showing a decreasing behavior. Meanwhile, it is noticed that the variations in the radiation parameter have no significant impact

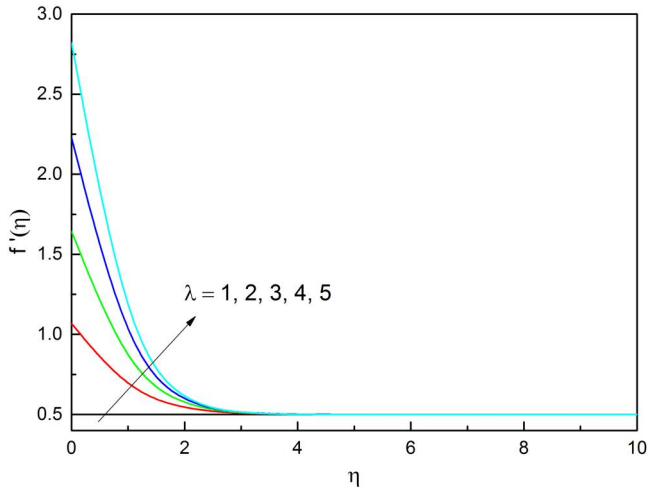


Figure 9. λ influence on $f'(\eta)$.

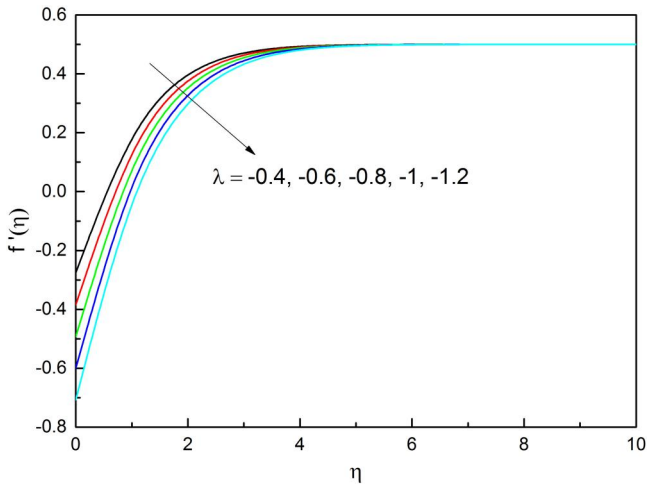


Figure 10. λ influence on $f'(\eta)$.

on the skin friction coefficient but it decreases the Nusselt number effectively. Furthermore, the higher values of δ reduce Cf_x whereas the Nusselt number increases significantly. A similar impact of the heat source/sink parameter is recorded where it is observed that the skin friction coefficient remains unaltered but the Nusselt number decreases.

6. Conclusion

The analysis of the flow of $MoS_2 - ZnO - SiO_2 - (H_2O + EG)$ ternary nanofluid over a stretching/shrinking thin needle was analyzed using a suitable mathematical model. The volumetric analysis was performed by implementing the RKF-45 numerical process. The obtained solutions were observed to be in good agreement with the existing sources and the outcomes were recorded in terms of graphs and tables. The designed mathematical model explains the thermal features of ternary nanofluid considering the effects of radiation and heat source/sink. Furthermore, the analysis was performed for both stretching and shrinking needle of radius $R(x)$. The hybrid nanofluid

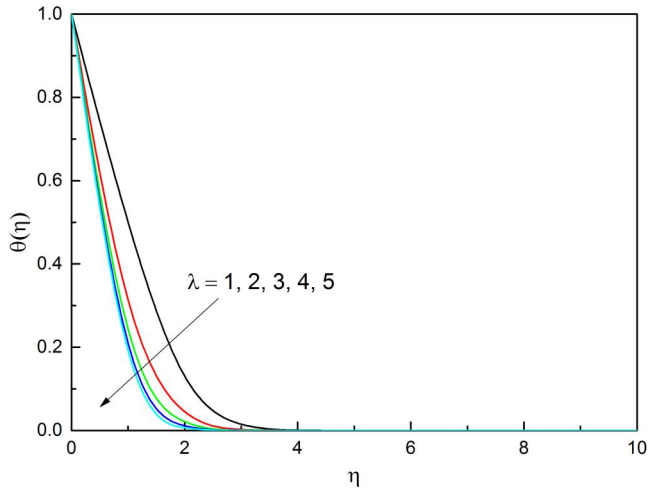


Figure 11. λ influence on $\theta(\eta)$.

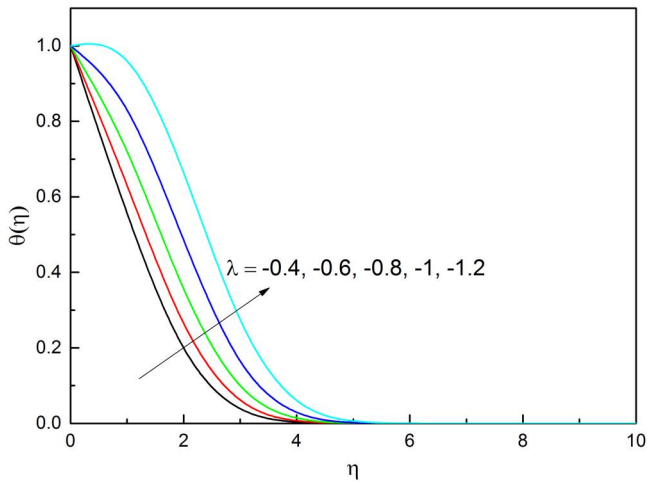


Figure 12. λ influence on $\theta(\eta)$.

Table 3. Variations of Cf_x and Nu_x for changes in the fluid flow parameters.

		$-Cf_x$	Nu_x			$-Cf_x$	Nu_x
ϕ	0.005	0.7243	0.9173	δ	0.1	0.7243	-0.0154
	0.01	0.6812	0.7679		0.2	0.8616	0.2569
	0.015	0.6274	6632		0.3	1.0345	0.5040
	0.02	0.5797	0.5048		0.4	1.2536	0.7095
	0.025	0.5547	0.3040		0.5	1.5329	0.8861
R	0.5	0.7243	1.3579	Q	-0.8	0.7243	2.318
	1	0.7243	1.0446		-0.4	0.7243	2.0266
	1.5	0.7243	0.8479		0	0.7243	1.6799
	2	0.7243	0.7121		0.4	0.7243	1.2355
	2.5	0.7243	0.6121		0.8	0.7243	0.5672

$ZnO - SiO_2 - (H_2O + EG)$ was assumed to be the base fluid which upon suspension of MoS_2 nanoparticles constituted the ternary nanofluid. Some of the major outcomes of the study are as follows:

- The velocity of the nanofluid decreases as the volume fraction of the nanoparticle is increased.
- The presence of more nanoparticles having higher thermal conductivity helps the nanofluid conduct more heat.
- The radiation causes the heat absorbed by the nanofluid to enhance significantly.
- As the heat source continuously emits the heat that is absorbed by the nanofluid, its temperature increases.
- Similar to the heat source, as the heat sink is strong the heat gets absorbed by it, and the overall temperature of the nanofluid is reduced.
- As the size of the needle is increased, the velocity at which the nanofluid flows is increased.
- As the needle is stretching the flow speed increases whereas the speed decreases as the needle is shrinking.

Ternary nanofluids have shown remarkable improvements in thermal conductivity compared to traditional heat transfer fluids. The presence of multiple types of nanoparticles in the fluid enhances the interfacial interaction and facilitates efficient heat transfer. While ternary nanofluids show great promise, it is important to note that further research and development are still needed to fully understand their behavior, optimize their properties, and address any potential challenges or limitations. Nonetheless, the importance of ternary nanofluids lies in their potential to revolutionize heat transfer and offer innovative solutions in various fields, leading to improved efficiency, performance, and sustainability.

Funding

The authors extend their appreciation to the Deanship of Scientific Research at King Khalid University for funding this work through large group Research Project Project under the grant number RGP2/107/44.

ORCID

Venkatesh Puneeth  <http://orcid.org/0000-0003-4470-6884>

References

- [1] H. Waqas et al., “Heat transfer analysis of hybrid nanofluid flow with thermal radiation through a stretching sheet: a comparative study,” *Int. Commun. Heat Mass Transf.*, vol. 138, pp. 106303, 2022. DOI: [10.1016/j.icheatmasstransfer.2022.106303](https://doi.org/10.1016/j.icheatmasstransfer.2022.106303).
- [2] R. Javadpour, S. Z. Heris, Y. Mohammadfam, and S. B. Mousavi, “Optimizing the heat transfer characteristics of MWCNTs and TiO₂ water-based nanofluids through a novel designed pilot-scale setup,” *Sci. Rep.*, vol. 12, no. 1, pp. 15154, 2022. DOI: [10.1038/s41598-022-19196-3](https://doi.org/10.1038/s41598-022-19196-3).
- [3] J. Mohammadpour, F. Salehi, A. Lee, and L. Brandt, “Nanofluid heat transfer in a microchannel heat sink with multiple synthetic jets and protrusions,” *Int. J. Therm. Sci.*, vol. 179, pp. 107642, 2022. DOI: [10.1016/j.ijthermalsci.2022.107642](https://doi.org/10.1016/j.ijthermalsci.2022.107642).
- [4] M. Yaseen, S. K. Rawat, A. Shafiq, M. Kumar, and K. Nonlaopon, “Analysis of heat transfer of mono and hybrid nanofluid flow between two parallel plates in a Darcy porous medium with thermal radiation and heat generation/absorption,” *Symmetry*, vol. 14, no. 9, pp. 1943, 2022. DOI: [10.3390/sym14091943](https://doi.org/10.3390/sym14091943).
- [5] B. Ali, S. A. Khan, A. K. Hussein, T. Thumma, and S. Hussain, “Hybrid nanofluids: significance of gravity modulation, heat source/sink, and magnetohydrodynamic on dynamics of micropolar fluid over an inclined surface via finite element simulation,” *Appl. Math. Comp.*, vol. 419, pp. 126878, 2022. DOI: [10.1016/j.amc.2021.126878](https://doi.org/10.1016/j.amc.2021.126878).
- [6] S. A. Khan et al., “Magnetic dipole and thermal radiation impacts on stagnation point flow of micropolar based nanofluids over a vertically stretching sheet: finite element approach,” *Processes*, vol. 9, no. 7, pp. 1089, 2021. DOI: [10.3390/pr9071089](https://doi.org/10.3390/pr9071089).

- [7] R. Anandika, V. Puneeth, S. Manjunatha, S. A. Shehzad, and M. Arshad, "Exploration of thermophoresis and Brownian motion effect on the bio-convective flow of Newtonian fluid conveying tiny particles: aspects of multi-layer model," *Proc. Inst. Mech. Eng., Part C*, vol. 236, no.19, pp.10185-10199, 2022.
- [8] X. Xin, A. M. Saeed, F. A. M. Al-Yarimi, V. Puneeth, and S. S. Narayan, "The flow analysis of Williamson nanofluid considering the Thompson and Troian slip conditions at the boundary," *Numer. Heat Transf.*, vol. Part A, pp. 1–17, 2023. DOI: [10.1080/10407782.2023.2212922](https://doi.org/10.1080/10407782.2023.2212922).
- [9] K. A. M. Alharbi et al., "Cattaneo–Christov heat flow model for copper–water nanofluid heat transfer under Marangoni convection and slip conditions," *Sci Rep.*, vol. 12, no. 1, pp. 5360, 2022. DOI: [10.1038/s41598-022-09275-w](https://doi.org/10.1038/s41598-022-09275-w).
- [10] S. A. Khan et al., "Study on the novel suppression of heat transfer deterioration of supercritical water flowing in vertical tube through the suspension of alumina nanoparticles," *Int. Commun. Heat Mass Transf.*, vol. 132, pp. 105893, 2022. DOI: [10.1016/j.icheatmasstransfer.2022.105893](https://doi.org/10.1016/j.icheatmasstransfer.2022.105893).
- [11] V. Puneeth, A. K. Baby, and S. Manjunatha, "The analogy of nanoparticle shapes on the theory of convective heat transfer of Au–Fe₃O₄ Casson hybrid nanofluid," *Heat Trans.*, vol. 51, no. 3, pp. 2586–2603, 2022. DOI: [10.1002/htj.22415](https://doi.org/10.1002/htj.22415).
- [12] A. Dezfulizadeh, A. Aghaei, A. H. Joshaghani, and M. M. Najafizadeh, "An experimental study on dynamic viscosity and thermal conductivity of water-Cu-SiO₂-MWCNT ternary hybrid nanofluid and the development of practical correlations," *Powder Technol.*, vol. 389, pp. 215–234, 2021. DOI: [10.1016/j.powtec.2021.05.029](https://doi.org/10.1016/j.powtec.2021.05.029).
- [13] A. Boroomandpour, D. Toghraie, and M. Hashemian, "A comprehensive experimental investigation of thermal conductivity of a ternary hybrid nanofluid containing MWCNTs-titania-zinc oxide/water-ethylene glycol (80: 20) as well as binary and mono nanofluids," *Synth. Met.*, vol. 268, pp. 116501, 2020. DOI: [10.1016/j.synthmet.2020.116501](https://doi.org/10.1016/j.synthmet.2020.116501).
- [14] Z. Said et al., "Synthesis, stability, density, viscosity of ethylene glycol-based ternary hybrid nanofluids: experimental investigations and model-prediction using modern machine learning techniques," *Powder Technol.*, vol. 400, pp. 117190, 2022. DOI: [10.1016/j.powtec.2022.117190](https://doi.org/10.1016/j.powtec.2022.117190).
- [15] J. Mohammed Zayan et al., "Investigation on rheological properties of water-based novel ternary hybrid nanofluids using experimental and Taguchi method," *Materials*, vol. 15, no. 1, pp. 28, 2021. DOI: [10.3390/ma15010028](https://doi.org/10.3390/ma15010028).
- [16] S. Manjunatha, V. Puneeth, B. Gireesha, and A. Chamkha, "Theoretical study of convective heat transfer in ternary nanofluid flowing past a stretching sheet," *J. Appl. Comp. Mech.*, vol. 8, no. 4, pp. 1279–1286, 2022.
- [17] S. Manjunatha, V. Puneeth, A. K. Baby, and C. Vishalakshi, "Examination of thermal and velocity slip effects on the flow of blood suspended with aluminum alloys over a bi-directional stretching sheet: the ternary nanofluid model," *Waves Random Complex Media*, pp. 1–18, 2022. DOI: [10.1080/17455030.2022.2056260](https://doi.org/10.1080/17455030.2022.2056260).
- [18] M. Arif, P. Kumam, W. Kumam, and Z. Mostafa, "Heat transfer analysis of radiator using different shaped nanoparticles water-based ternary hybrid nanofluid with applications: a fractional model," *Case Stud. Therm. Eng.*, vol. 31, pp. 101837, 2022. DOI: [10.1016/j.csite.2022.101837](https://doi.org/10.1016/j.csite.2022.101837).
- [19] F. Shahzad et al., "Second-order convergence analysis for hall effect and electromagnetic force on ternary nanofluid flowing via rotating disk," *Sci Rep.*, vol. 12, no. 1, pp.18769, 2022. DOI: [10.1038/s41598-022-23561-7](https://doi.org/10.1038/s41598-022-23561-7).
- [20] V. Puneeth, S. Manjunatha, K. Ganesh Kumar, and M. Gnaneswara Reddy, "Perspective of multiple slips on 3D flow of Al₂O₃–TiO₂–CuO/H₂O ternary nanofluid past an extending surface due to non-linear thermal radiation," *Waves Random Complex Media*, pp. 1–19, 2022. DOI: [10.1080/17455030.2022.2041766](https://doi.org/10.1080/17455030.2022.2041766).
- [21] X. Wang et al., "Heat transfer and flow characteristic of a flat confined loop thermosyphon with ternary hybrid nanofluids for electronic devices cooling," *Appl. Therm. Eng.*, vol. 221, pp. 119758, 2023.
- [22] W. Ahmed et al., "Heat transfer growth of sonochemically synthesized novel mixed metal oxide ZnO + Al₂O₃ + TiO₂/DW based ternary hybrid nanofluids in a square flow conduit," *Renew. Sustain. Energy Rev.*, vol. 145, pp. 111025, 2021. DOI: [10.1016/j.rser.2021.111025](https://doi.org/10.1016/j.rser.2021.111025).
- [23] J. Hasnain and N. Abid, "Numerical investigation for thermal growth in water and engine oil-based ternary nanofluid using three different shaped nanoparticles over a linear and nonlinear stretching sheet," *Numer. Heat Transf.*, vol. Part A, pp. 1–12, 2022.
- [24] V. Puneeth et al., "Implementation of modified Buongiorno's model for the investigation of chemically reacting rGO-Fe₃O₄-TiO₂-H₂O ternary nanofluid jet flow in the presence of bio-active mixers," *Chem. Phys. Lett.*, vol. 786, pp. 139194, 2022. DOI: [10.1016/j.cplett.2021.139194](https://doi.org/10.1016/j.cplett.2021.139194).
- [25] B. Ali, S. Hussain, Y. Nie, S. A. Khan, and S. I. R. Naqvi, "Finite element simulation of bioconvection Falkner–Skan flow of a Maxwell nanofluid fluid along with activation energy over a wedge," *Phys. Scr.*, vol. 95, no. 9, pp. 095214, 2020. DOI: [10.1088/1402-4896/abb0aa](https://doi.org/10.1088/1402-4896/abb0aa).
- [26] M. Rehman et al., "Soret and dufour influences on forced convection of cross radiative nanofluid flowing via a thin movable needle," *Sci. Rep.*, vol. 12, no. 1, pp. 18666, 2022. DOI: [10.1038/s41598-022-23563-5](https://doi.org/10.1038/s41598-022-23563-5).

- [27] A. Shafiq, A. B. Çolak, and T. N. Sindhu, "Modeling of solet and DuFour's convective heat transfer in nano-fluid flow through a moving needle with artificial neural network," *Arabian J. Sci. Eng.*, vol. 48, no. 3, pp. 2807-2820, 2023.
- [28] T. Nazar, M. Bhatti, and E. E. Michaelides, "Hybrid (Au-TiO₂) nanofluid flow over a thin needle with magnetic field and thermal radiation: dual solutions and stability analysis," *Microfluid Nanofluid*, vol. 26, no. 1, pp. 1-12, 2022. DOI: [10.1007/s10404-021-02504-0](https://doi.org/10.1007/s10404-021-02504-0).
- [29] M. Yasir, A. Ahmed, and M. Khan, "Carbon nanotubes based fluid flow past a moving thin needle examine through dual solutions: stability analysis," *J. Electrochem. Energy Convers. Storage*, vol. 48, pp. 103913, 2022. DOI: [10.1016/j.est.2021.103913](https://doi.org/10.1016/j.est.2021.103913).
- [30] A. Khan et al., "Bio-convective and chemically reactive hybrid nanofluid flow upon a thin stirring needle with viscous dissipation," *Sci. Rep.*, vol. 11, no. 1, pp. 8066, 2021. DOI: [10.1038/s41598-021-86968-8](https://doi.org/10.1038/s41598-021-86968-8).
- [31] V. Puneeth, S. Manjunatha, O. Makinde, and B. Gireesha, "Bioconvection of a radiating hybrid nanofluid past a thin needle in the presence of heterogeneous-homogeneous chemical reaction," *J. Heat Transf.*, vol. 143, no. 4, pp. 042502, 2021.
- [32] A. Akinshilo, F. Mabood, and A. Ilegbusi, "Heat generation and nonlinear radiation effects on MHD Casson nanofluids over a thin needle embedded in porous medium," *Int. Commun. Heat Mass Transf.*, vol. 127, pp. 105547, 2021. DOI: [10.1016/j.icheatmasstransfer.2021.105547](https://doi.org/10.1016/j.icheatmasstransfer.2021.105547).
- [33] S. Jahan, M. Ferdows, M. Shamshuddin, and K. Zaimi, "Effects of solar radiation and viscous dissipation on mixed convective non-isothermal hybrid nanofluid over moving thin needle," *J. Adv. Res. Micro Nano Eng.*, vol. 3, no. 1, pp. 1-11, 2021.
- [34] A. U. Yahya et al., "Thermal characteristics for the flow of Williamson hybrid nanofluid (Mos₂+ Zno) based with engine oil over a stretched sheet," *Case Stud. Therm. Eng.*, vol. 26, pp. 101196, 2021. DOI: [10.1016/j.csite.2021.101196](https://doi.org/10.1016/j.csite.2021.101196).
- [35] K. Das, B. Sutradhar, and P. K. Kundu, "Impact of nonlinear radiation on an unsteady magneto hybrid nanofluid flow over an upward/downward rotating disk," *Numer. Heat Transf. Part A*, pp. 1-18, 2023. DOI: [10.1080/10407782.2023.2228477](https://doi.org/10.1080/10407782.2023.2228477).
- [36] S. Ontela, V. Musala, S. E. Ahmed, and T. Thumma, "Optimization and sensitivity analysis on axisymmetric motile microorganism flow of viscoelastic nanofluid over a spinning circular disk with a central composite model," *Numer. Heat Transf. Part A*, pp. 1-26, 2023. DOI: [10.1080/10407782.2023.2251088](https://doi.org/10.1080/10407782.2023.2251088).
- [37] M. Shamshuddin, I. L. Animasaun, S. O. Salawu, and P. S. Rao, "Dynamics of ethylene glycol conveying MWCNTs and ethylene glycol conveying SWCNTs: significant joule heating and thermal radiation," *Numer. Heat Transf. Part A*, pp. 1-20, 2023. DOI: [10.1080/10407782.2023.2195130](https://doi.org/10.1080/10407782.2023.2195130).
- [38] A. Mishra and G. Pathak, "A comparative analysis of Mos₂-Sio₂/H₂O hybrid nanofluid and Mos₂-Sio₂-Go/H₂O ternary hybrid nanofluid over an inclined cylinder with heat generation/absorption," *Numer. Heat Transf. Part A*, pp. 1-30, 2023. DOI: [10.1080/10407782.2023.2228483](https://doi.org/10.1080/10407782.2023.2228483).
- [39] M. Qasim, Z. H. Khan, W. A. Khan, and I. Ali Shah, "Mhd boundary layer slip flow and heat transfer of ferrofluid along a stretching cylinder with prescribed heat flux," *PLoS One*, vol. 9, no. 1, pp. e83930, 2014. DOI: [10.1371/journal.pone.0083930](https://doi.org/10.1371/journal.pone.0083930).
- [40] M. Suleman et al., "A numerical simulation of silver-water nanofluid flow with impacts of Newtonian heating and homogeneous-heterogeneous reactions past a nonlinear stretched cylinder," *Symmetry*, vol. 11, no. 2, pp. 295, 2019. DOI: [10.3390/sym11020295](https://doi.org/10.3390/sym11020295).